Received: 10 November 2023 | Accepted: 16 December 2023

DOI: 10.1097/HC9.0000000000000374

ORIGINAL ARTICLE

OPEN

The role of sinusoidal endothelial cells and TIMP1 in the regulation of fibrosis in a novel human liver 3D NASH model

Sander van Riet[1] | **Anais Julien**[2] | **Andrea Atanasov**[1,3] | **Åsa Nordling**[1] | **Magnus Ingelman-Sundberg**[1]

[1]Department of Physiology and Pharmacology, Section of Pharmacogenetics, Karolinska Institutet, Stockholm, Sweden

[2]Department of Cell and Molecular Biology, Karolinska Institutet, Stockholm, Sweden

[3]Department of Physiology, Faculty of Pharmacy, University of Belgrade, Belgrade, Serbia

Correspondence
Sander van Riet, Department of Physiology and Pharmacology, Karolinska Institutet, SE-171 77 Stockholm, Sweden; 468-524 877 35.
Email: sander.van.riet@ki.se

Abstract

Background: The prevalence of NAFLD is rapidly increasing. NAFLD can progress to NASH, fibrosis, cirrhosis, and HCC, which will soon become the main causes of liver transplantation. To date, no effective drug for NASH has been approved by the Food and Drug Administration. This is partly due to the lack of reliable human in vitro models. Here, we present a novel human liver spheroid model that can be used to study the mechanisms underlying liver fibrosis formation and degradation.

Methods and Results: Such spheroids, which contain hepatocytes, stellate cells, KC, and LSECs, spontaneously develop fibrosis that is exacerbated by treatment with free fatty acids. Conditioned medium from activated LSECs caused similar activation of fibrosis in spheroids containing primary human hepatocyte and NPCs, indicating the action of soluble mediators from the LSECs. Spheroids containing LSECs treated with free fatty acids produced tissue inhibitor of metalloproteinases inhibitor 1, a matrix metalloproteinases inhibitor important for fibrosis progression. Tissue inhibitor of metalloproteinases inhibitor 1 knockdown using siRNA led to a reduction in collagen and procollagen accumulation, which could be partially rescued using a potent matrix metalloproteinases inhibitor. Interestingly, tissue inhibitor of metalloproteinases inhibitor 1 was found to be expressed at higher levels, specifically in a subtype of endothelial cells in the pericentral region of human fibrotic livers, than in control livers.

Conclusion: Potential anti-NASH drugs and compounds were evaluated for their efficacy in reducing collagen accumulation, and we found differences in specificity between spheroids with and without LSECs. This new

Abbreviations: COL1A1, collagen type I alpha 1 chain; CYP, cytochrome P450; ECM, extracellular matrix; FBS, fetal bovine serum; FFA, free fatty acids; LSEC-CM, liver sinusoidal endothelial cell-conditioned medium; MMP, matrix metalloproteinases; NPC, nonparenchymal cell; PHH, primary human hepatocyte; siRNA, Small interfering RNA; TIMP1, tissue inhibitor of metalloproteinases inhibitor 1; VCAM-1, vascular cell adhesion molecule 1.

Supplemental Digital Content is available for this article. Direct URL citations are provided in the HTML and PDF versions of this article on the journal's website, www.hepcommjournal.com.

This is an open access article distributed under the terms of the Creative Commons Attribution-Non Commercial-No Derivatives License 4.0 (CCBY-NC-ND), where it is permissible to download and share the work provided it is properly cited. The work cannot be changed in any way or used commercially without permission from the journal.

Copyright © 2024 The Author(s). Published by Wolters Kluwer Health, Inc. on behalf of the American Association for the Study of Liver Diseases.

human NASH model may reveal novel mechanisms for the regulation of liver fibrosis and provide a more appropriate model for screening drugs against NASH.

INTRODUCTION

NAFLD is the most common liver disease worldwide, affecting up to 30% of the population, and its prevalence is expected to continue to increase.[1] NAFLD is an umbrella term for a range of diseases that can start with simple steatosis and progress to NASH, fibrosis, cirrhosis, and ultimately HCC.[2] NASH is characterized by a further increase in steatosis, inflammation, and accumulation of extracellular matrix (ECM) produced mainly by activated hepatic stellate cells (HSC).[3] NASH is the fastest growing indication for liver transplantation and is expected to soon be the most common.[4] Currently, there are no clinically approved drugs for the treatment of NASH or appropriate biomarkers for NASH to develop preventive or treatment strategies.[5] This is partly because of our incomplete understanding of the pathophysiology of human NASH, particularly in the early stages of the disease.

Liver sinusoidal endothelial cells (LSECs) line the walls of the hepatic sinusoids. Their location between the liver parenchyma and blood originating from the intestine and systemic circulation, as well as their permeable morphology, have made them gatekeepers of the hepatic microenvironment. LSECs produce nitric oxide, which regulates vascular tone and contributes to the maintenance of HSC quiescence.[6] In both acute and chronic injuries, LSECs are activated and lose their protective function, increase the secretion of pro-inflammatory cytokines, and facilitate immune infiltration through the expression of chemoattractants and adhesive molecules.[7,8] This activation impedes the exchange of substances and oxygenation of the surrounding parenchyma, which, together with the decrease in nitric oxide and the increase in inflammatory mediators and profibrotic mediators, activates HSC. One class of these profibrotic molecules is the TIMP metallopeptidase (TIMP) inhibitor, which plays a role in various processes but is mainly known to control the activity of enzymatic matrix metalloproteinases (MMPs) and promote HSC survival.[9–11]

The central role of LSECs in sinusoidal paracrine signaling between different liver cells and their role in immune surveillance makes the maintenance and restoration of LSECs' activity essential for the prevention or alleviation of liver disease. Targeting LSECs or signaling pathways involved in LSECs' activation may be a promising part in the strategy for the treatment or prevention of NASH. However, the research and development of targeted LSEC therapies has been hampered by the lack of suitable preclinical human models and overreliance on less transferable rodent models. A model with integrated endothelial cells has been published by InSphero AG.[12] However, to our knowledge, no human in vitro model has revealed any role of LSEC in the progression of fibrosis.

Our lab has previously developed a spheroid culture setup[13,14] that has been further developed into a NASH model based on cocultures of hepatocytes and the crude fraction of nonparenchymal cells (NPCs).[15,16] Here, we present a novel human in vitro spheroid model, including hepatocytes, stellate cells, and LSECs, which can be used to investigate the role of these cells in the development, progression, and treatment of liver fibrosis. Using this model, we describe the LSEC-related signaling pathways and mechanisms involved in the development and degradation of fibrosis, with tissue inhibitor of metalloproteinases inhibitor 1 (TIMP1) playing an important role. Based on the altered properties of this more complex in vitro NASH model compared to previous variants, we propose that the system may represent a more appropriate in vitro system for analyses of mechanisms of regulation of liver fibrosis and for screening the efficacy and mechanism of novel anti-NASH drug candidates.

METHODS

Cell culture

Primary human hepatocytes (PHH), crude fractions of NPC, and LSECs were obtained from LONZA or KaLy-Cell. The donor characteristics and supporting information are presented in Table 1. Spheroids were cultured as described.[13,15] Briefly, PHH were seeded in 96-well Corning Costar Ultra-Low Attachment Plates (Merck, Kenilworth, NY) or in 96-Well Nunclon Sphera U-Shaped-Bottom Microplate plates (Thermo Fisher, Waltham, MA) in the following compositions: (i) PHH alone (monoculture), (ii) PHH/NPC (coculture), and (iii) PHH/NPC/LSEC (triple culture). For different spheroid compositions, PHH/NPC and PHH/NPC/LSEC were seeded at ratios of 1500/375 and 1500/375/200 cells per well, respectively. Spheroids were seeded in William's E medium supplemented with 2 mM L-glutamine (Sigma-Aldrich, Saint Louis, MO), 100 U/mL penicillin (Sigma-Aldrich), 100 µg/mL streptomycin (Sigma-Aldrich), 100 nM dexamethasone (Sigma-Aldrich), ITS X-100 (Thermo Fisher), and 10% fetal bovine serum (FBS; Thermo Fisher). Following spheroid formation (~5 d), the cells

TABLE 1 Donor characteristics

PHH	NPC	LSEC	Source	Cat. Nu.	Age	Sex	Ethnicity	BMI	PNPLA3 rs738409	PNPLA3 rs2294918
X	—	—	KLC	S1506T	47	Female	Caucasian	20,7	Het.	WT
X	—	—	Lonza	HUM190171	48	Female	Caucasian	22,4	Het.	WT
X	—	—	Lonza	HUM201221	51	Female	African American	21,7	WT	Hom.
—	X	—	KLC	S1493	63	Male	Caucasian	—	WT	WT
—	—	X	Lonza	180070ECP2	52	Female	Caucasian	35,42	—	—
—	—	X	Lonza	180071ECP2	52	Female	Hispanic	44,4	—	—
—	—	X	Lonza	180072ECP2	59	Female	Caucasian	40	—	—

Abbreviations: BMI, body mass index; KLC, KaLy-Cell; NPC, nonparenchymal cell; PHH, primary human hepatocyte; PNPLA3, Patatin-like phospholipase domain-containing protein 3; WT, Wild Type.

were refreshed every 2–3 days with complete William's E medium without FBS. Treatment of the spheroids with different compounds or 480 μM free fatty acids ([FFA] in a 1:1 ratio of oleic acid and palmitic acid [Sigma-Aldrich]) was initiated on day 7 after seeding. The spheroids were treated for 7 days and harvested on day 14. Spheroids were cultured in 100 μL of medium under standard cell culture conditions at 37°C in a humidified incubator with 5% CO_2.

LSEC-Conditioned medium

LSECs (1×10^5) were seeded per well in a 6-well plate (Thermo Fisher) in complete William's E medium with 10% FBS. After 24 hours, the cells were washed with PBS to remove excess FBS, and dead cells and medium were replaced with William's E medium without FBS. After 6–7 days, the medium was collected and used immediately or stored at −20°C. liver sinusoidal endothelial cell-conditioned medium (LSEC-CM) was diluted with William's E medium without FBS in a 1:1 ratio.

Two-D staining on poly-L-lysine coating of slides

Glass immunohistochemistry adhesive slides (Histolab, Askim, Sweden) were coated with 50 μL droplets of 0.01% (w/v) poly-L-lysine (Sigma-Aldrich) and left at room temperature until all liquid evaporated. Cells (1×10^4) were collected in 50 μL medium + 10% FBS and placed on the poly-L-lysine-coated area until all the liquid evaporated. After evaporation, the cells were fixed with 4% paraformaldehyde and stained, as described below.

siRNA-Mediated TIMP1 silencing

Small interfering RNA (siRNA) knockdown of TIMP1 was performed on the day of seeding according to the manufacturer's instructions. The siRNA (TIMP1 siRNA, Silencer Select, Thermo Fisher) and its scrambled control (Thermo Fisher) were diluted in OptiMEM (Thermo Fisher) to a final concentration of 50 nM. Additionally, Lipofectamine RNAiMAX (Thermo Fisher) was diluted with OptiMEM to obtain a final volume of 0.2 μL of lipofectamine RNAiMAX per well. Following a 5-minute incubation, both mixtures were carefully mixed in a 1:1 ratio. The mixture was then incubated at room temperature for 20 minutes. The transfection siRNA–lipid complex solution was mixed with the cell suspension during seeding.

Cell viability

Cell viability was measured using the CellTiter Glo Luminescent Cell Viability Assay kit (Promega, Madison, WI) according to the manufacturer's instructions. First, 80 μL of 100 μL medium was removed from each well, and 25 μL of reconstituted assay reagent was added. The spheroids were then incubated for 20 minutes in the dark at 37°C. The luminescence signal was measured using a MicroBeta LumiJET 2460 Microplate Counter (Perkin Elmer, Waltham, MA) in white flat-bottom 96-well plates. Data are represented as relative luminescent units, with every data point representing the average of 4 spheroids.

RNA isolation and cDNA synthesis and qPCR

RNA isolation was performed using the QIAzol method as described.[16] To ensure sufficient RNA, at least 48 spheroids were lysed per condition. RNA concentration was determined using a Qubit 4 fluorometer (Thermo Fisher). Up to 500 ng of RNA was used to generate cDNA with SuperScript III reverse transcriptase (Thermo Fisher) using a SimpliAmp Thermal Cycler (Thermo Fisher) according to the manufacturer's protocol. Quantitative PCR reactions were performed using 2X TaqMan Universal PCR mix (Thermo Fisher) on a 7500 Fast Real-Time PCR system (Applied Biosystems, Waltham, MA) with 20X TaqMan probes (Supplemental Table S1, http://links.lww.com/HC9/A782). Gene expression was

analyzed using the delta-delta Ct method (2−ΔΔCt), with TATA-binding protein and glyceraldehyde 3-phosphate dehydrogenase as reference genes.

Immunofluorescence staining

The spheroids were fixed for 2 hours at room temperature in 4% paraformaldehyde and subsequently dehydrated in 30% sucrose for at least 2 days at 4°C. The spheroids were embedded and frozen using Tissue-Tek OCT (Sakura Finetek, Alphen aan den Rijn, The Netherlands) and sectioned at 8 μm using a NX70 Cryostat (Thermo Fisher). Spheroid sections were blocked using 5% BSA and 0.25% Triton X-100 in PBS (PBT, Sigma-Aldrich) for 2 hours at room temperature. A list of the antibodies is provided in Supplemental Table S2, http://links.lww.com/HC9/A782.

The spheroid sections were stained with a primary antibody diluted in PBT overnight at 4°C. The slides were washed with PBS 3 times. Next, the secondary antibody diluted in PBT was added and incubated for 2 hours at room temperature in the dark. The slides were then washed 3 times with PBS. The slides were mounted with ProLong Gold Antifade containing DAPI (Thermo Fisher) and imaged using an Olympus IX73 inverted microscope (Olympus, Tokyo, Japan). Images were analyzed using the Fiji software version 2.12.0. For quantification, the integrated density of the respective staining was normalized to the area stained with DAPI. Every data point represents the average fluorescence intensity of at least 10 imaged spheroids.

NileRed (Sigma-Aldrich) staining was performed as described.[13]

ELISA

The Human Pro-Collagen I α1 DuoSet ELISA kit (R&D Systems) and Human TIMP1 DuoSet ELISA kit (R&D Systems) were used according to the manufacturer's instructions. ELISA was performed on the supernatants of spheroids collected from random wells on day 14.

Human cytokine antibody array

RayBio Human Cytokine Array C5 (RayBiotech, Norcross, GA) was performed according to the manufacturer's instructions to detect the cytokine expression in LSEC-CM. Mix of 3 batches of LSEC-CM was used for the assay.

Single-cell RNA-sequencing analysis

Human single-cell RNA-sequencing analyses were performed using the Rstudio (v2022.07.1) software and the Seurat R package (v4.3.0).[17,18] Human datasets were collected from the Gene Expression Omnibus public database (accession number: GSE192742). The datasets used in the analyses are shown in Supplemental Figure 2, http://links.lww.com/HC9/A784, and Supplemental Table S3, http://links.lww.com/HC9/A782. For each dataset, cells expressing more than 500–5000 genes and expressing less than 10% of the mitochondrial genes were retained for analysis. Each matrix was processed following the classical steps of the Seurat package using default parameters. The matrices were then integrated using the harmony package (v0.1.1), following default parameters.[19] Dimensional reduction was performed using the first 20 principal components and clustering was performed using a resolution of 0.5. Two consecutive subclustering steps were performed to extract endothelial and stellate cells. First, nonendothelial, nonhepatocyte, and nonstellate cells were extracted based on cluster identity. Leftover immune cells and erythrocytes were removed based on gene expression; that is, cells expressing PTPRC < 0.2 and GYPA < 0.2 were kept. Second, hepatocytes were removed based on cluster identity to retain only the endothelial and stellate cells. Dimensional reduction was performed using the first 10 principal components, and a resolution of 0.3 was used for the clustering.

Cluster identity was assessed by plotting the known gene expression and lineage scores for each cell type. The lineage score is defined as the arithmetic mean of a given list of genes (Supplemental Table S4, http://links.lww.com/HC9/A782).[20]

Statistical analysis

Statistical analysis was performed using GraphPad Prism version 9.0.0 (GraphPad Software, San Diego, CA), and graphs are shown as the mean and SEM. Statistical analysis of differences was performed using a paired two-sided *t*-test and comparing each condition to the appropriate control. Data are shown as the mean ± SEM. $*p < 0.05$; $**p < 0.01$; $***p < 0.01$; $****p < 0.01$.

Ethical approval

All research was conducted in accordance with both the Declarations of Helsinki and Istanbul, all research was approved by the appropriate ethics and/or institutional review committee(s), and written consent was given in writing by all subjects. PHH, NPC, and LSEC were obtained from commercially available sources and required no ethical approval from the Karolinska Institute. Ethical approval for the donors was obtained from the project partners at KaLy-Cell. Copies of documentation from Lonza regarding the written consent of donors were obtained from the respective companies. Liver tissue samples were obtained from

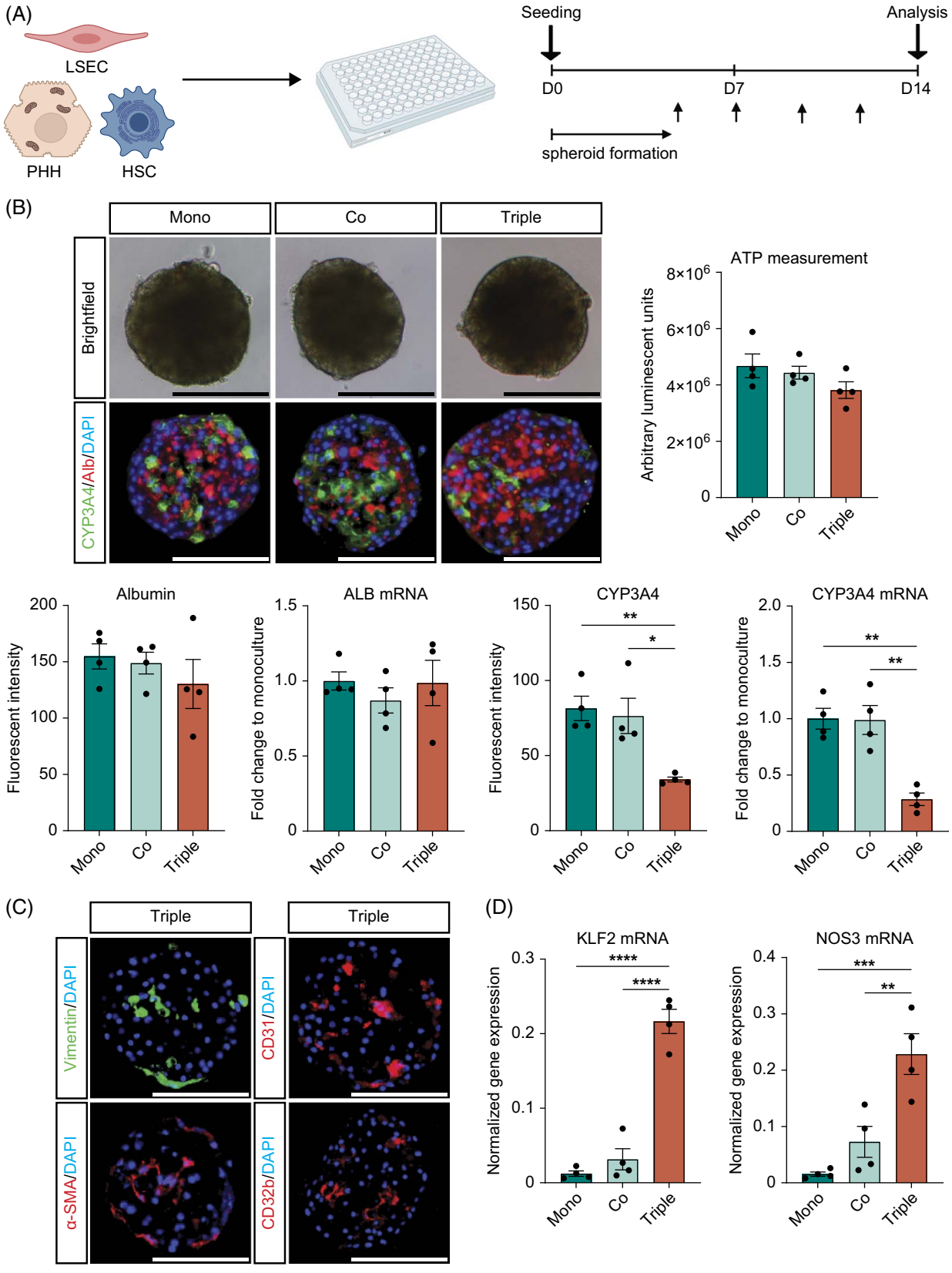

FIGURE 1 LSEC inclusion in the hepatic spheroids. (A) Schematic overview of the seeding and refresh schedule of the spheroid cultures. Figure made using Biorender. (B) Representative bright-field and immunofluorescent images of spheroids of different compositions on day 14 after seeding. ATP measurement of the different spheroid compositions on day 14 (n = 4 independent experiments). Analysis of albumin and CYP3A4 mRNA expressions and protein levels of different spheroid compositions on day 14 (n = 4 independent experiments). (C) Triple-culture spheroids

on day 14 stained for general mesenchymal markers (vimentin, α-smooth muscle actin) and LSEC markers (CD32b, CD31). (D) Expression of endothelial genes *KLF2* and *NOS3* in spheroids of different compositions on day 14 (n = 4 independent experiments). Scalebar is 100 μm. Abbreviations: KLF2, Krüppel-like factor 2; NOS3, nitric oxide synthase 3.

the Liver Bank[21] and approved by the Regional Ethical Committee (D:nr 2017/269-31).

RESULTS

Inclusion of LSEC into the hepatic spheroids

The feasibility of integrating LSECs into hepatic spheroids and the effects of LSECs on the hepatic phenotype were evaluated. Hepatic spheroids with different cell compositions were generated: (i) primary human hepatocytes alone (PHH; monoculture), (ii) PHH +nonparenchymal cells (NPC; coculture), and (iii) PHH +NPC+LSEC (triple culture). In the triple cultures, PHH/NPC/LSECs were seeded at a ratio of 1500/375/200 cells in ultralow attachment plates, where they aggregated and formed spheroids after ~5 days and were subsequently analyzed after 14 days in culture (Figure 1A, B). The hepatocyte markers albumin (periportal) and cytochrome P450 3A4 (CYP3A4) (perivenous) were analyzed at the mRNA and protein levels (Figure 1B). The protein levels of CYP3A4 and albumin prior to seeding (t = 0) were evaluated by staining the cells on poly-L-lysine–coated slides and were found to be ~50% of PHH CYP3A4+ (Supplemental Figure 1A, http://links.lww.com/HC9/A783). Both the mRNA and protein concentrations of albumin remained constant between spheroids of different compositions during cultivation. In contrast, the mRNA and protein expressions of CYP3A4 decreased significantly in the triple cultures containing LSECs compared to the monoculture and coculture conditions. This decrease was not accompanied by a decrease in spheroid viability, indicating that LSECs cause a cytokine-mediated decrease of CYP3A4 in perivenous hepatocytes.[22] In addition, spheroids were analyzed for mesenchymal cell (vimentin and α-smooth muscle actin) and LSEC (CD32b and CD31) markers (Figure 1C and Supplemental Figure 1B, C, http://links.lww.com/HC9/A783). Vimentin and α-smooth muscle actin were only detected in coculture and triple culture, whereas CD32b and CD31 were predominantly detected in LSEC-containing spheroids. In addition, markers for nonactivated LSECs Krüppel-like factor 2 and nitric oxide synthase 3 were almost exclusively expressed in triple cultures (Figure 1D). LSECs at $t = 0$ showed CD32b expression in ~90% of the cells (Supplemental Figure 1B, http://links.lww.com/HC9/A783), whereas the proportion of CD31-positive cells was proportionally higher in the spheroids. This is consistent with the phenotypic changes observed during LSEC activation.

Development of steatosis and fibrosis in the hepatic spheroids

It has previously been shown that FFAs are a physiologically relevant inducer of ECM protein deposition in the coculture spheroid model composed of hepatocytes and NPCs.[15] Since various NPCs, especially LSECs, possess scavenger receptors, FFA uptake between spheroids of different compositions was compared. Following spheroid formation, the different cultures were treated with FFA (480 μM) from days 7 to 14 (Figure 2A). The total lipid accumulation in the different spheroid compositions treated with FFA was increased compared to medium, but there was no difference in uptake between the spheroid compositions (Figure 2B).

Evaluation of collagen 1A1 (COL1A1) production revealed undetectable COL1A1 in monocultures, increased COL1A1 production in the cocultures caused by FFA, and high FFA-independent accumulation in the triple cultures containing LSECs (Figure 2C). A similar pattern, measuring procollagen 1A1 (pro-COL1A1) accumulation, was observed in the medium of coculture and triple culture. However, only in the triple culture, FFA increased the pro-COL1A1 accumulation, suggesting that the production of pro-COL1A1 is increased more than can be processed to mature COL1A1. Lysyl oxidase plays a role in the processing and crosslinking of collagen fibers, and lysyl oxidase expression increased upon FFA treatment in both the coculture and triple culture and fibronectin in the triple cultures (Figure 2D). In contrast, nitric oxide synthase 3 and Krüppel-like factor 2 expressions decreased in triple cultures upon treatment with FFA (Figure 2E). These findings are consistent with the phenotypic changes observed in LSECs following activation.

LSEC secreted mediators

COL1A1 deposition and pro-COL1A1 accumulation were higher in the triple cultures compared to coculture spheroids, indicating that the presence of LSECs in the spheroids aggravated the model and increases ECM production. This effect can principally be mediated through cell-cell interactions and LSECs derived secreted mediators. To investigate this, LSEC-CM was produced and used to stimulate cocultures (Figure 3A). After 7 days, LSEC-CM caused a similar change in

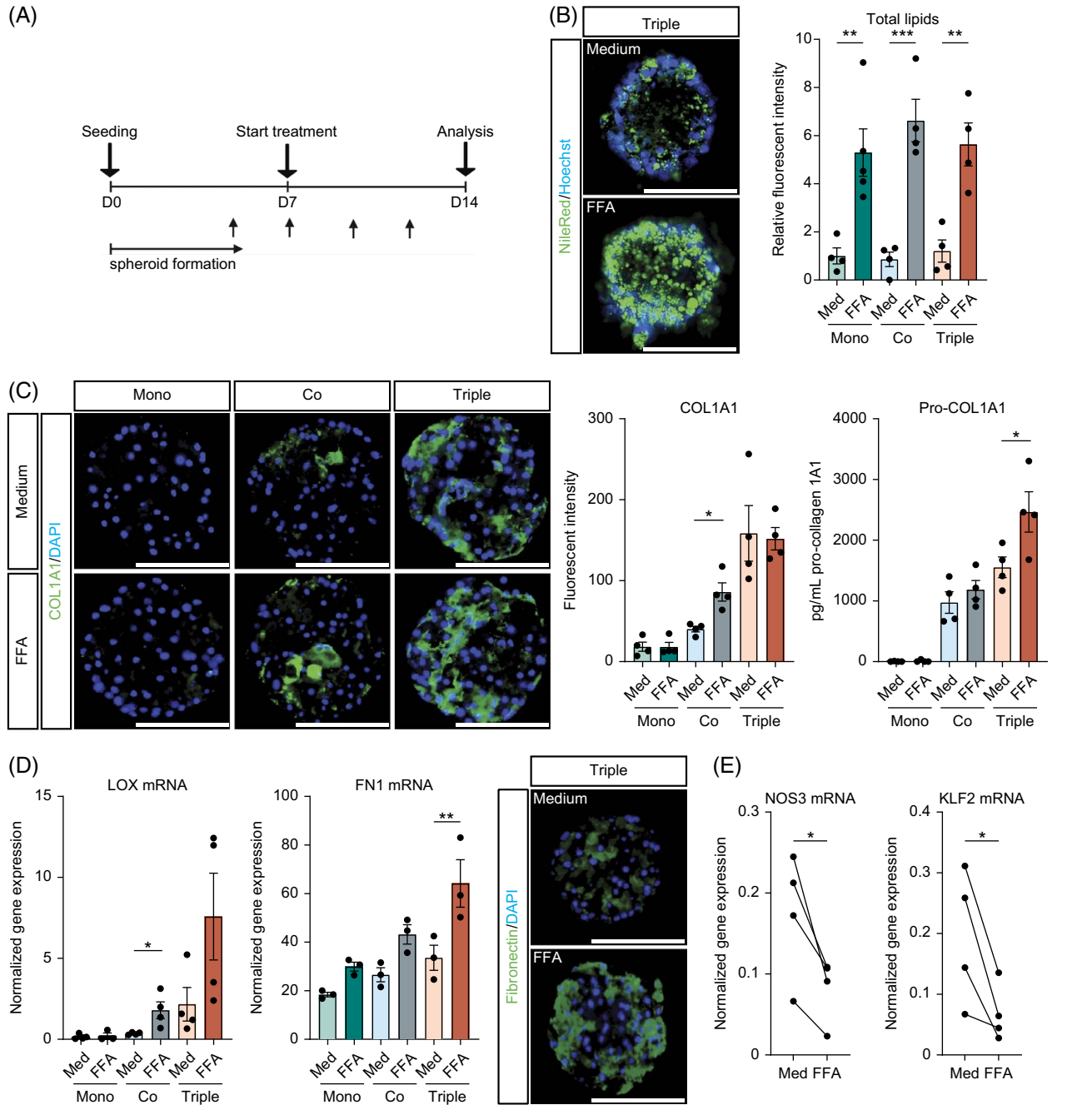

FIGURE 2 Triple-culture spheroid response to free fatty acids. (A) Schematic overview of the seeding, treatment, and refresh schedule of the spheroid cultures. Figure made using Biorender. (B) Representative images of triple-culture spheroids with or without FFA treatment. Quantification of NileRed staining of spheroids of different compositions treated for 7 days with FFA on day 14 (n = 4 independent experiments). (C) Representative images of COL1A1 staining of spheroids of different compositions with or without FFA treatment on day 14. Quantification of COL1A1 staining of the different spheroid compositions and pro-COL1A1 ELISA of medium collected on day 14 (n = 4 independent experiments). (D) *LOX* and *FN1* gene expressions and representative images of fibronectin staining on triple cultures with and without FFA treatment. (E) Expression of the endothelial markers *NOS3* and *KLF2* in triple cultures with and without FFA treatment (n = 4 independent experiments). Scalebar is 100 μm. Abbreviations: COL1A1, collagen type I alpha 1 chain; FFA, free fatty acids; KLF2, Krüppel-like factor 2; LOX, lysyl oxidase; NOS3, nitric oxide synthase 3.

hepatocyte phenotype as observed by LSECs in the culture (Figure 3B-D). Albumin mRNA and protein expressions remained stable, whereas CYP3A4 mRNA and protein levels decreased upon LSEC-CM treatment, likely caused by an LSEC-mediated cytokine-induced loss of CYP3A4 in the perivenous hepatocyte fraction. In a previous study, we analyzed the effect of different cytokines on the expression of drug absorption, distribution, metabolism, and excretion genes in liver spheroids.[22] Based on the data presented, we here

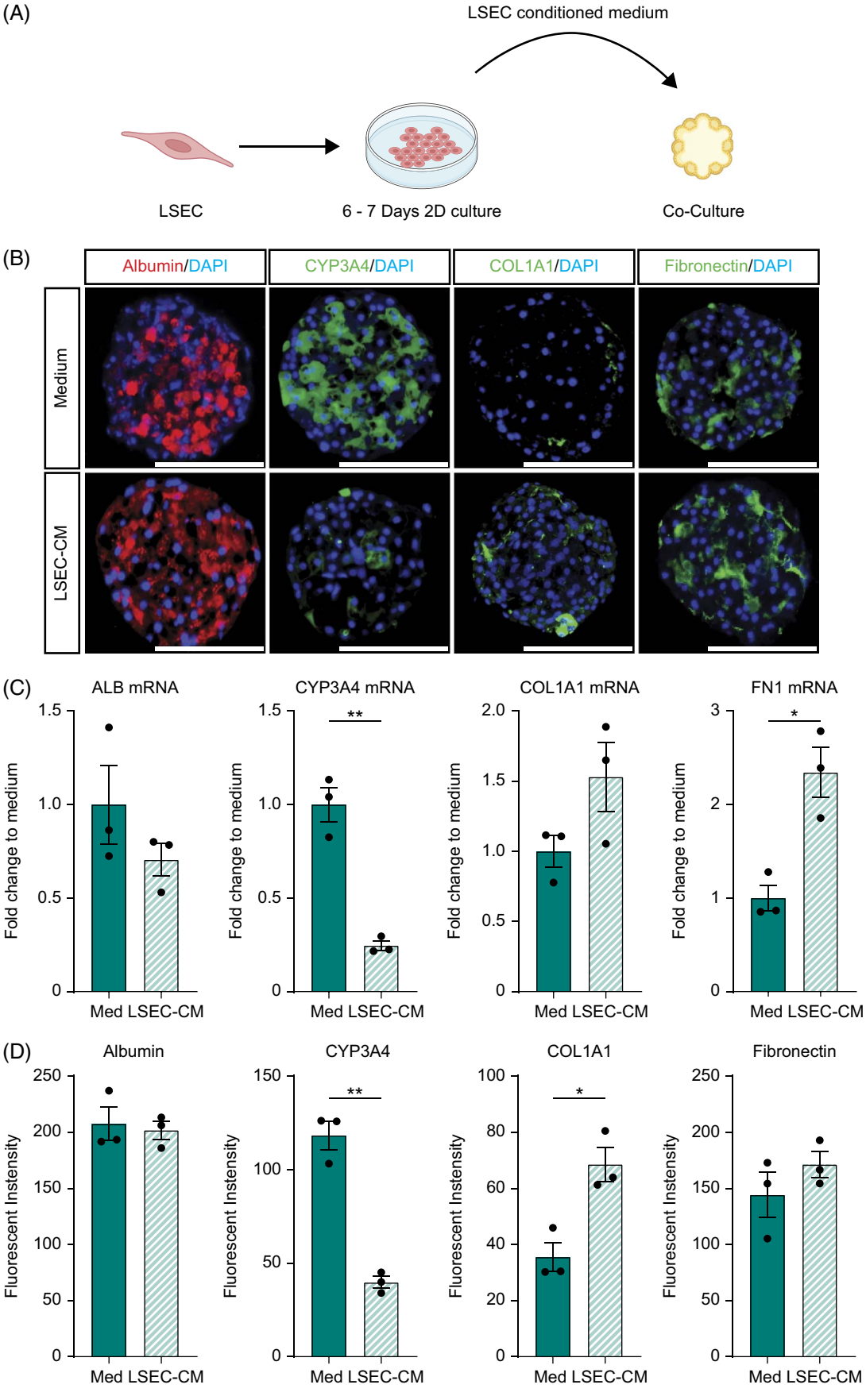
(A)
LSEC conditioned medium
LSEC
6 - 7 Days 2D culture
Co-Culture
(B)
Albumin/DAPI
CYP3A4/DAPI
COL1A1/DAPI
Fibronectin/DAPI
Medium
LSEC-CM
(C)
ALB mRNA
CYP3A4 mRNA
COL1A1 mRNA
FN1 mRNA
Fold change to medium
Med LSEC-CM
(D)
Albumin
CYP3A4
COL1A1
Fibronectin
Fluorescent Instensity
Med LSEC-CM

FIGURE 3 LSEC-conditioned medium can induce a fibrotic phenotype in cocultures. (A) Schematic overview LSEC-CM generation and treatment of cocultures. Figure made using Biorender. (B) Representative images of cocultures cultured in standard culture medium or in LSEC-CM: standard culture medium 1:1. Scalebar is 100 μm. (C) Analysis of albumin, CYP3A4, COL1A1, and FN1 mRNA expressions in standard medium and LSEC-CM: standard medium 1:1. (D) albumin, CYP3A4, COL1A1, and FN1 protein levels as assessed of immunofluorescent images of spheroids in standard medium and LSEC-CM: standard medium 1:1 on day 14 (n = 3 independent experiments). Abbreviations: COL1A1, collagen type I alpha 1 chain; FN1, fibronectin; LSEC-CM, liver sinusoidal endothelial cell-conditioned medium.

measured IL-6 in the culture medium (Supplemental Figure 2, http://links.lww.com/HC9/A784). Higher levels of IL-6 were found in the triple-culture medium compared to the monoculture or coculture mediums (Supplemental Figure 2A, http://links.lww.com/HC9/A784). Treatment of monoculture spheroids with IL-6 and/or the IL-6 inhibitor LMT-28 resulted in a significant decrease or increase in CYP3A4 mRNA and protein (Supplemental Figure 2B and C, http://links.lww.com/HC9/A784). LSEC-CM also caused an increase in COL1A1 and FN1 expressions in the cocultures, similar to that observed in triple cultures, whereas IL-6 alone did not increase COL1A1 accumulation (Supplemental Figure 2D, http://links.lww.com/HC9/A784). Taken together, these results suggest that activated LSECs can induce fibrosis in coculture and triple-culture spheroids through the production of different soluble mediators including IL-6 rather than by cell-cell contact-mediated mechanisms.

TIMP1 expression in hepatic spheroids

LSECs play a central role in the communication between different cells in the sinusoidal space by secreting signaling compounds.[23] A publicly available RNA-sequencing database was used to identify potentially interesting mediators secreted by LSECs (Figure 4A-C, Supplemental Figure 3A-C, http://links.lww.com/HC9/A785).[24] First, the CD45+ cells were excluded and all CD45− cells were used for clustering, revealing clusters of hepatocytes, stellate cells, and LSECs. Next, the hepatocyte clusters were excluded and LSECs and stellate cells were selected for further subclustering. We then analyzed the differentially expressed genes in the different LSEC clusters for genes related to fibrosis and that are secreted. TIMP1 was selected as a fibrosis-associated gene of interest (Supplemental Table S5, http://links.lww.com/HC9/A782). In the total CD45− population, we only observed TIMP1 expression in the endothelial and stellate cell populations and not in the hepatocytes (Figure 4D). In the mesenchymal population, we found high TIMP1 expression in a subset of LSECs as well as in a subset of stellate cells (Figure 4E).

Members of the TIMP family can inhibit MMP, thereby contributing to fibrosis. The expression of TIMP family genes (TIMP1-3) was analyzed in spheroid cultures with and without FFA treatment (Figure 4F). Overall, *TIMP1* was the most highly expressed, particularly in the triple cultures at the protein and mRNA levels (Figure 4F-I, Supplemental Figures 3D, http://links.lww.com/HC9/A785), and the expression of all TIMP genes was induced by FFA in spheroids containing LSECs. TIMP1 was detected in the triple culture using immunofluorescence and western blotting and was also detected in the culture medium using ELISA (Figure 4G-I Full Western blot images can be found in Supplemental Materials 1, http://links.lww.com/HC9/A828). Additionally, a human cytokine screen was performed on the LSEC-CM as validation (Figure 4J, Supplemental Figures 3E, http://links.lww.com/HC9/A785). We observed high levels of IL-6, IL-8, TIMP1, TIMP2 as well as different chemokines and growth factors. The human cytokine array further demonstrates that the LSECs are capable of producing TIMP1. Finally, TIMP1 was co-stained with vimentin and CD31, and TIMP1/vimentin and TIMP1/CD31 double positive cells could be observed (Figure 4K). Taken together, these results support the finding that TIMP1 is produced by the LSECs and in the triple-culture spheroids, which can be further induced by FFA treatment of the spheroid system.

TIMP1 expression in human liver samples

To assess the significance of TIMP1 protein expression in the triple cultures, we analyzed the expression of TIMP family genes in liver samples (Supplemental Table S6, http://links.lww.com/HC9/A782). Two independent pathologists classified the samples as control or fibrotic based on the morphology of the Hematoxylin and eosin-stained liver sections. Overall, we found a similar relative expression pattern for the 3 different TIMPs as in the spheroids, with TIMP1 being the most highly expressed (Figure 5A). We analyzed the expression of TIMP1 in control and fibrotic liver samples by immunofluorescence and found that TIMP1 was selectively expressed in the vicinity of the large vessels radiating into the parenchyma (Figure 5B), with the samples classified as fibrotic showing higher TIMP1 staining around the vessels than the control livers. As only a selection of the large vessels were positive for TIMP1, we used adjacent liver sections and the pericentral hepatocyte marker cytochrome P450 family 2 subfamily E member 1 to show that TIMP1 expression was localized predominantly around the central vein (Figure 5C). The available data suggest that TIMP1 is produced in the central region of the hepatic lobule and its expression is increased in fibrotic livers.

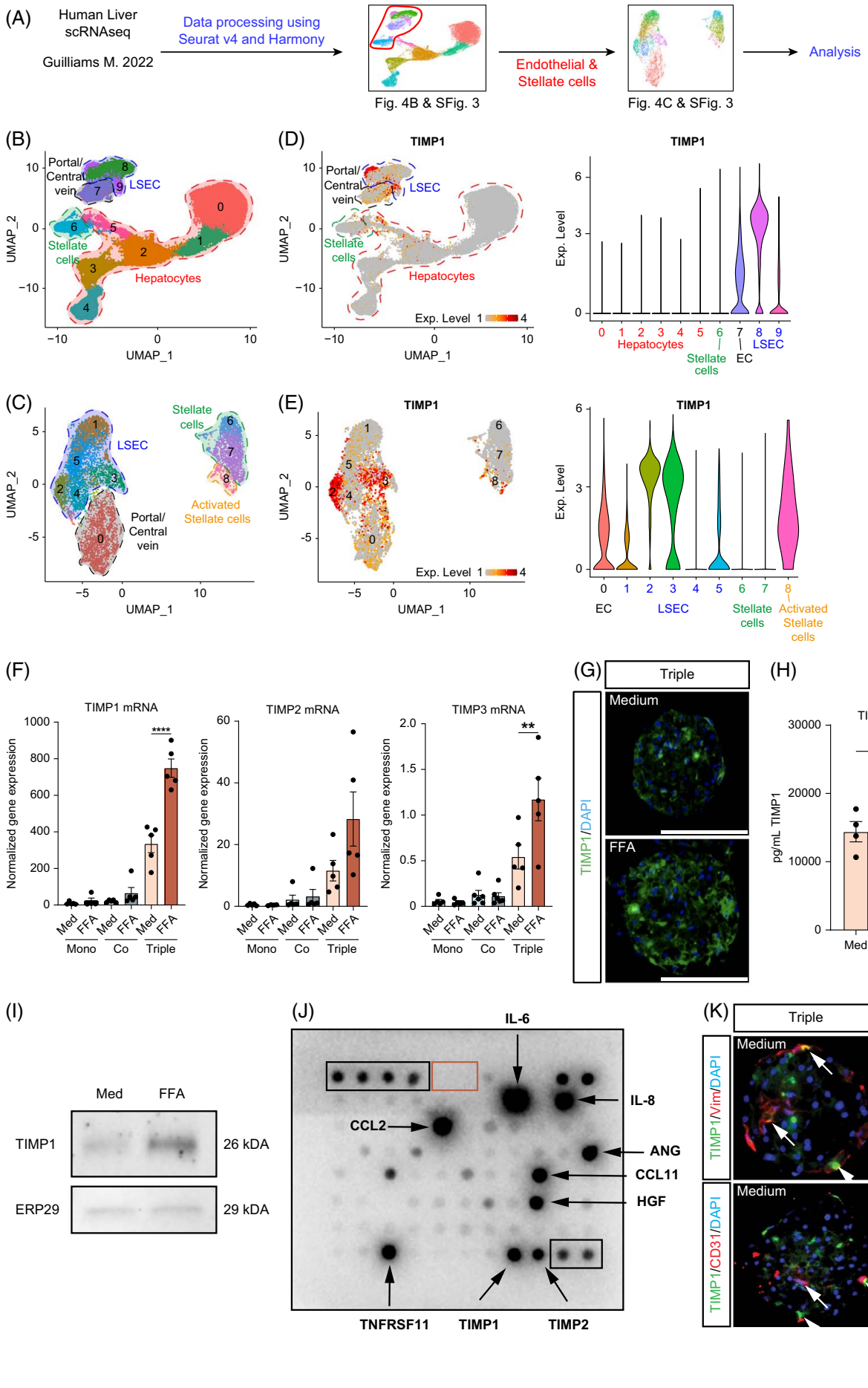
(A)
Human Liver scRNAseq
Guilliams M. 2022
Data processing using Seurat v4 and Harmony
Fig. 4B & SFig. 3
Endothelial & Stellate cells
Fig. 4C & SFig. 3
Analysis
(B)
Portal/ Central vein
LSEC
Stellate cells
Hepatocytes
UMAP_1
UMAP_2
(D)
TIMP1
Exp. Level
(C)
Activated Stellate cells
(E)
Exp. Level
(F)
TIMP1 mRNA
TIMP2 mRNA
TIMP3 mRNA
Normalized gene expression
Med
FFA
Mono
Co
Triple
(G)
Triple
Medium
FFA
TIMP1/DAPI
(H)
TIMP1
pg/mL TIMP1
(I)
Med
FFA
TIMP1
ERP29
26 kDa
29 kDa
(J)
IL-6
IL-8
CCL2
ANG
CCL11
HGF
TNFRSF11
TIMP1
TIMP2
(K)
Triple
Medium
TIMP1/Vim/DAPI
TIMP1/CD31/DAPI

FIGURE 4 TIMP1 expression in liver and spheroids. (A) Schematic overview of analysis scheme. Data were retrieved from the liver atlas (Guilliams M. 2022) and reanalyzed. (B) UMAP projection of CD45− cell types found in the nanospheres: endothelial cells, stellate cells, and hepatocytes. (C) UMAP projection of the subclustering of endothelial cells and stellate cells. (D) FeaturePlot (left) and violinplot (right) of TIMP1 expression in the total CD45− cell population. (E) FeaturePlot (left) and violinplot (right) of TIMP1 expression in endothelial and stellate cells. (F) mRNA expression of TIMP1, −2, and −3 in spheroids of different compositions with and without FFA treatment on day 14 (n = 5 independent experiments). (G) TIMP1 protein immunofluorescence staining in the triple-culture spheroids with and without FFA at day 14. Scalebar is 100 μm. (H) TIMP1 ELISA of triple-culture spheroid medium with and without FFA treatment on day 14. (I) Western blot of TIMP1 protein in triple-culture spheroids with and without FFA at day 14. (J) Human cytokine array was used to screen the LSEC-CM. Black boxes are the positive control and the red boxes the negative controls. Black arrows indicate the most prevalent proteins (Full layout can be found in Supplemental Figure 3E, http://links.lww.com/HC9/A785). (K) Staining of TIMP1 combined with vimentin or CD31 in untreated triple-culture spheroids. White arrows indicate double positive cells. Abbreviations: FFA, free fatty acids; LSEC-CM, liver sinusoidal endothelial cell-conditioned medium; TIMP1, tissue inhibitor of metalloproteinases inhibitor 1; UMAP, uniform manifold approximation and projection.

Targeting TIMP1 in hepatic spheroids

To determine the extent to which TIMP1 plays a role in collagen accumulation in the spheroid model, we used siRNA to suppress its expression. Spheroids in triple cultures transfected with TIMP1 siRNA (siRNA directed against TIMP1) with or without FFA treatment showed greatly reduced gene and protein expressions compared to the scrambled control (siCTRL) (Figure 6A-C). FFA treatment increased TIMP1 gene expression and protein levels, whereas no significant effect of FFA was observed in spheroids treated with TIMP1 siRNA. These spheroids were then examined for COL1A1 deposition and pro-COL1A1 production (Figure 6D, E). The siRNA directed against TIMP1 spheroids showed less accumulation of COL1A1 in the spheroid or pro-COL1A1 in the medium on day 14. In addition, FFA treatment did not result in increased collagen production in either case.

The reduction in collagen accumulation by the down-regulation of TIMP1 suggests that TIMP-mediated inhibition of MMP might be important for the fibrotic phenotype of LSEC-containing spheroids. Screening of liver samples for MMPs revealed the highest expression of MMP2 and MMP9 (Figure 6F), which are enzymes classified as gelatinases that can degrade type I collagen.[25] In the triple spheroids, MMP2 was most abundant and induced by FFA, whereas MMP9 was expressed to a lesser extent (Figure 6F). As MMP2 mRNA expression was highest in both the liver samples and the spheroids, MMP2 protein was measured in the different spheroid compositions with and without FFA treatment (Figure 6G). In the medium condition, pro-MMP2 was found in the coculture and triple-culture spheroids. Upon FFA treatment, cleaved MMP2 was observed in all conditions with the highest expression in the triple culture. To determine whether the decrease in COL1A1 under the conditions of TIMP1 silencing was due to the increased activity of MMPs, the siTIMP triple spheroids were treated with the MMP inhibitor ARP-100 (Figure 6H). ARP-100 treatment increased the deposition of COL1A1 in the siRNA directed against TIMP1-treated spheroids, suggesting a regulatory role of MMP in the inhibitory effect of TIMP1 (Figure 6I).

Screening of anti-NASH compounds in coculture and triple-culture spheroids

The coculture and triple-culture spheroids were used to screen for different anti-NASH drugs directed at a variety of targets (Supplemental Table S7, http://links.lww.com/HC9/A782). Coculture and triple-culture spheroids were treated with FFA and potential anti-NASH agents for 7 days, and the accumulation of COL1A1, pro-COL1A1, and TIMP1 was measured on day 14 (Figure 7A-C). As shown previously, the ALK5 inhibitor SB-525334 and pan-peroxisome proliferator–activated receptors agonist lanifibranor reduced COL1A1 accumulation in the cocultures.[15] In the triple cultures, SB-525334 and lanifibranor, as well as the vascular cell adhesion protein-1 (VCAM-1) inhibitor AGI-1067, showed a reduction in COL1A1 accumulation. VCAM-1 is an adhesion protein that is elevated on LSECs or HSC during NASH and can promote inflammation and fibrosis (Supplemental Figure 4, http://links.lww.com/HC9/A786).[26,27] BI-1467335, a vascular adhesion protein-1 inhibitor did not show any effect on either culture or both molsidomine and mevastatin.

Levels of pro-COL1A1 were slightly reduced in both coculture and triple culture after treatment with AGI-1067 and SB-525334, whereas no decrease was observed in lanifibranor-treated spheroids (Figure 7B). TIMP1 mRNA expression in the triple cultures decreased after treatment with AGI-1067, lanifibranor, and SB-525334 (Figure 7C). Taken together, these data suggest that fibrotic regulation in cocultures differs from that in the novel triple model, leading to differential sensitivity to NASH inhibitors, which is important information with respect to the choice of human NASH model for mechanistic analysis of the regulation of fibrosis, as well as for future screening of new drug candidates.

DISCUSSION

In this study, we developed an improved human liver spheroid fibrosis model and highlighted the contribution of LSECs in fibrosis progression. We found an important

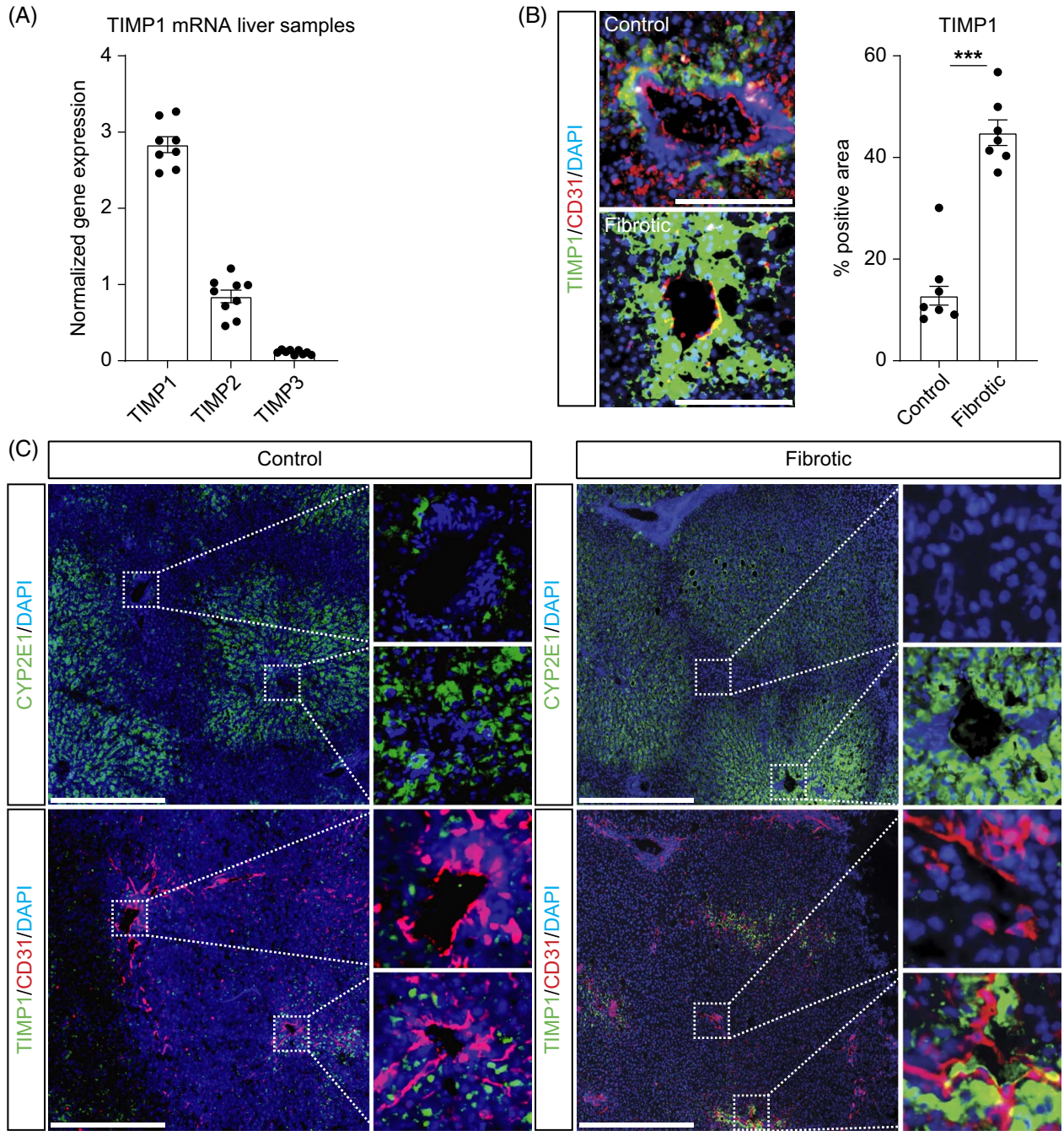

FIGURE 5 TIMP1 expression in human liver samples. (A) mRNA expression analysis of TIMP1, −2, and −3 in 9 different human liver samples. (B) Fluorescent images of large vessels in tissue sections of control and fibrotic samples stained for TIMP1 and CD31. Scalebar is 100 μm. Quantification of TIMP1 area surrounding TIMP1-positive vessels in control and fibrotic samples. Each data point represents the average positive area per sample. (C) Adjacent tissue sections stained for CYP2E1 or TIMP1/CD31 in control and fibrotic liver samples. Scalebar is 500 μm. Abbreviation: CYP2E1, cytochrome P450 family 2 subfamily E member 1; TIMP1, tissue inhibitor of metalloproteinases inhibitor 1.

contribution of LSECs to the development of fibrosis in the system and a crucial role in the regulation of TIMP1 and MMPs in fibrosis development and degradation. TIMP1 was found to be expressed only in a subclass of LSECs present around larger pericentral vessels. The improved spheroid model has a different sensitivity to specific anti-NASH compounds as compared to the coculture model and would allow studies of novel mechanisms behind the formation and degradation of liver fibrosis and be suitable for the identification of more specific anti-NASH drug candidates.

Our previously published liver spheroid model of fibrosis contained primary human hepatocytes and the crude fraction of NPCs.[15] The NPC fraction contains predominantly HSCs, as well as some KCs and some LSECs, although the ratio varies between batches and

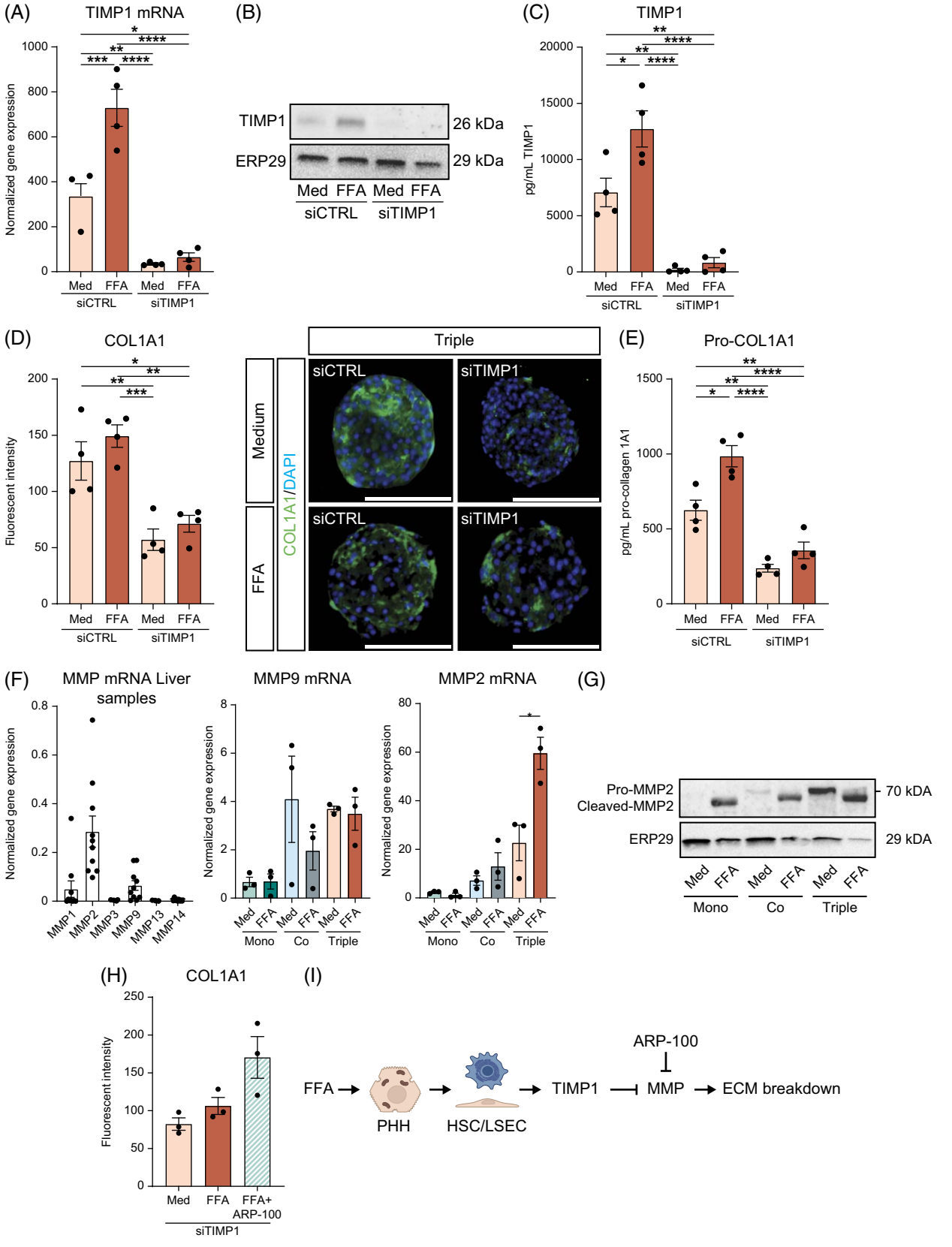

FIGURE 6 Role of TIMP1 during fibrosis in the triple-culture spheroids. (A) TIMP1 mRNA and (B) protein levels in triple-culture spheroids transfected with siCTRL or siTIMP1 treated with or without FFA. (C) Quantification of TIMP1 in the culture medium by ELISA harvested on day 14 (n = 4 independent experiments) (D) COL1A1 staining quantification in triple-culture spheroids transfected with siCTRL or siTIMP1 treated with or without FFA. Scalebar is 100 μm. (E) Quantification of pro-COL1A1 in the culture medium by ELISA harvested on day 14

(n = 4 independent experiments). (F) mRNA expression analysis of various MMPs in human liver samples (n = 9 liver donor RNA samples). MMP2 and MMP9 mRNA expressions in spheroids of different compositions (n = 3 independent experiments). (G) Western blot analysis of MMP2 protein levels in different spheroid compositions with and without FFA treatment on day 14. (H) Quantification of COL1A1 staining of samples transfected with siTIMP1 treated with FFA and ARP-100 (100 μM) (n = 3 independent experiments). (I) Schematic overview of ECM degradation interactions. Figure made using Biorender. Abbreviations: COL1A1, collagen type I alpha 1 chain; ECM, extracellular matrix; FFA, free fatty acids; MMP, matrix metalloproteinases; siCTRL, control siRNA; siTIMP1, siRNA directed against TIMP1; TIMP1, tissue inhibitor of metalloproteinases inhibitor 1.

donors. The inclusion of additional LSECs into the spheroids revealed the presence of endothelial markers for the duration of the culture. CD32b was highly expressed initially in the spheroids, but decreased proportionally in the spheroids, while CD31-positive cells became more abundant, consistent with LSEC activation.[28] The spheroids contained hepatocytes originating from either the perivenous or periportal liver region, and the cellular phenotypes persisted for long periods of cultivation (Figure 1B). Cytochrome P450 enzymes are strongly influenced by cytokines and are mainly downregulated in diseases causing systemic inflammation.[29,30] The monoculture or coculture spheroid model has been found to be very useful for studying the mechanisms and consequences of cytokine exposure to the liver.[22] In this triple culture system, we observed a very important and rapid pro-inflammatory cytokine–mediated downregulation, for example, the perivenously localized *CYP3A4* and *UGT2B10* genes. During hepatic LSEC activation, a LSEC-mediated pro-inflammatory cascade was observed[31] and the observed decrease of CYP3A4 expression in hepatocytes within the triple cultures was likely due to the LSEC-mediated release of such cytokines. IL-6 levels were found to be high in the LSEC-CM (Figure 4J) and produced in the triple culture spheroids (Supplemental Figure 2, http://links.lww.com/HC9/A784) and was found to decrease CYP3A4 mRNA and protein expressions (Supplemental Figure 2, http://links.lww.com/HC9/A784), whereas the inhibition of IL-6 by LMT-28 increased CYP3A4 expression.

The spheroids of the triple cultures reliably accumulated COL1A1 and pro-COL1A1 proteins, which could be enhanced by challenging spheroids with FFA. Moreover, genes associated with fibrosis were upregulated after FFA treatment, whereas nitric oxide synthase 3 and Krüppel-like factor 2 were reduced. Using LSEC-CM, we found that the conditioned medium containing soluble mediators from the activated LSEC induced a fibrosis-like phenotype in the cocultures and decreased CYP3A4 expression, compatible with elevated levels of pro-inflammatory cytokines, whereas albumin expression in hepatocytes in the periportal region remained stable.

The TIMP family is closely associated with fibrosis, as it regulates the balance between ECM deposition and accumulation by targeting MMP proteins and influencing HSC survival.[10,32–34] TIMP1 plays a role in the development and progression of NAFLD/NASH.[10,35] TIMP1 is a secreted compound that can be detected systemically in patients, but only in advanced disease states.[36,37] TIMP1 knockdown in the triple-culture spheroids resulted in a decrease in COL1A1 accumulation in the spheroid as well as a decrease in pro-COL1A1 accumulation in the medium. Inhibition of MMP partially restored COL1A1 accumulation in spheroids. Analysis of a publicly available RNA-sequencing database revealed that TIMP1 is highly expressed in subsets of HSC and LSEC,[24] which was confirmed for the LSEC using a human cytokine array. These TIMP1-producing cells were localized around the perivenous regions in large vessels (Figure 2), that is, in a region known to be most vulnerable to NAFLD-related steatosis and inflammation.[38] Increased TIMP1 staining in these cells was observed in livers classified as fibrotic compared to control livers. Taken together, these data support the idea that targeting LSEC activity can contribute to the reduction of fibrosis.

SB-525334 caused a decrease in COL1A1 accumulation in the triple cultures and cocultures, whereas the extent of inhibition by lanifibranor was somewhat lower in the triple cultures (Figure 7). Interestingly, the VCAM-1 inhibitor AGI-1067 decreased COL1A1 in the triple cultures, but not in cocultures. VCAM-1 is increased in the liver during NASH and in response to inflammation and can promote further inflammation and fibrosis.[26] VCAM-1 facilitates macrophage and leukocyte invasion into tissues, which is not encapsulated in the spheroid cultures. The mechanism by which AGI-1067 reduces COL1A1 accumulation remains unclear, but it could have endothelial-selective antioxidant and anti-inflammatory activities.[39] BI-1467335, which targets vascular adhesion protein-1 and is also restricted to LSECs, did not show any effect on COL1A1 accumulation in coculture or triple culture. A summary of the model, including the action of the tested effective drugs, is shown in Figure 8.

However, this model has some limitations. While it was possible to determine the relative contribution of TIMP1 or other factors to the progression of fibrosis in the spheroids, it was not possible to accurately determine the contribution of each cell type to COL1A1 accumulation due to the spheroid structure. Therefore, all cell types were susceptible to drug and siRNA interventions. Furthermore, the cell-cell interactions within the spheroid that might play a role in protein and gene regulation are difficult to mimic with this setup. PHH donors were selected for the Patatin-like phospholipase domain-containing protein 3 polymorphism

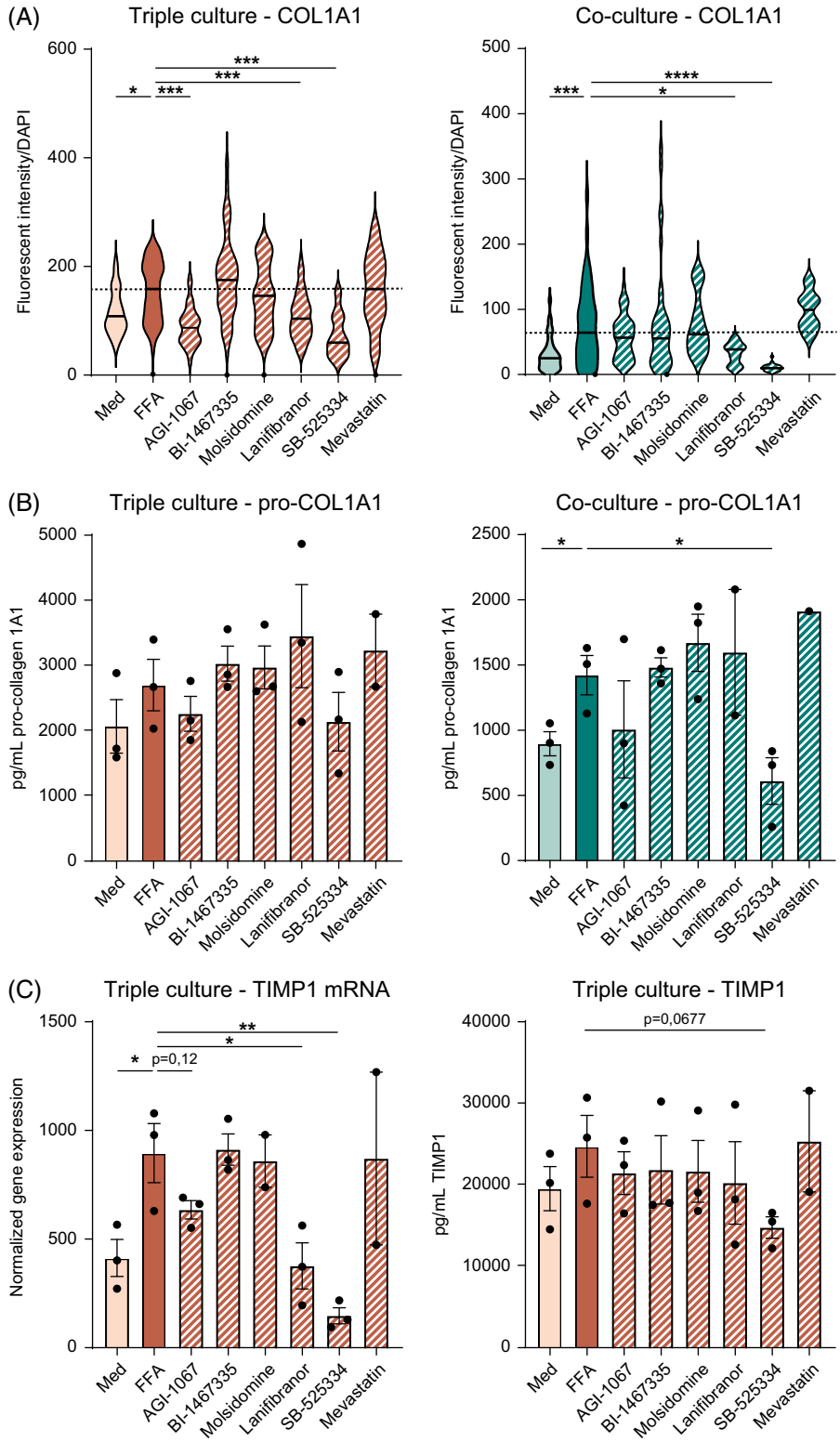

FIGURE 7 Screening of anti-NASH compounds in coculture and triple-culture spheroids. (A) COL1A1 protein levels in coculture and triple-culture spheroids treated with FFA together with potential anti-NASH compounds on day 14. (B) pro-COL1A1 levels in the medium of coculture and triple-culture spheroids treated with FFA together with potential anti-NASH compounds on day 14. (C) TIMP1 mRNA expression and TIMP1 protein levels in culture medium of coculture and triple-culture spheroids treated with FFA together with potential anti-NASH compounds on day 14. Abbreviations: COL1A1, collagen type I alpha 1 chain; FFA, free fatty acids; TIMP1, tissue inhibitor of metalloproteinases inhibitor 1.

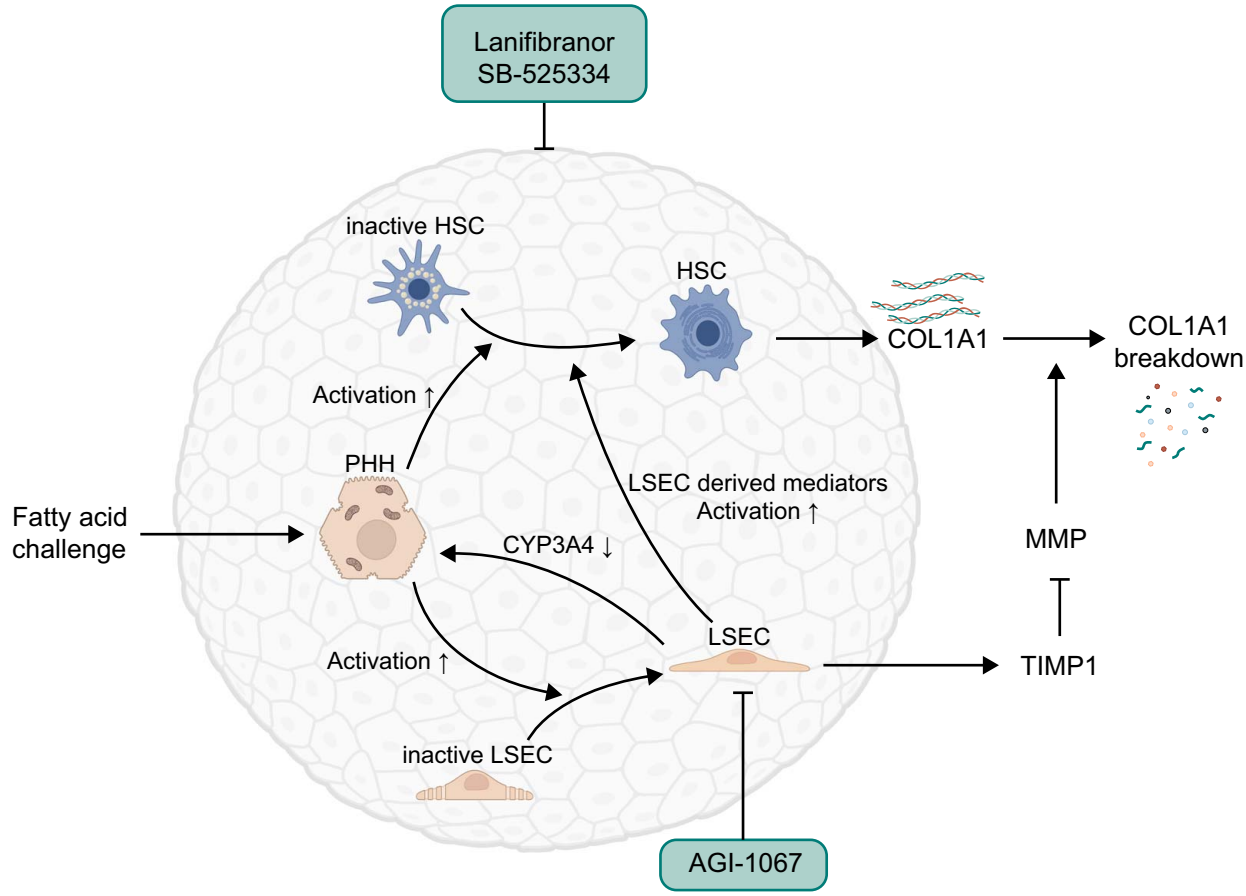

FIGURE 8 Schematic overview of triple-culture COL1A1 accumulation and interventions. Schematic overview of the different cell types in the triple-culture spheroids and the proposed interaction leading to increased COL1A1 accumulation. Fatty acids challenge of the triple-culture spheroid leads to steatosis and a stress signaling cascade in the PHH. Stress signals to the surrounding cells activate the HSC and LSEC, leading to an increase in TIMP1 and COL1A1 production. Soluble mediators produced by the activated LSEC decrease CYP3A4 expression in PHH and lead, partly through inhibition of MMPs by TIMP1, to an increase in COL1A1 accumulation. The anti-NASH compounds lanifibranor and SB-525334 target all cell types in the spheroid, whereas AGI-1067 specifically affects the LSEC. Figure made using Biorender. Abbreviations: COL1A1, collagen type I alpha 1 chain; CYP3A4, cytochrome P450 3A4; MMP, matrix metalloproteinases; PHH, primary human hepatocyte; TIMP1, tissue inhibitor of metalloproteinases inhibitor 1.

I148M, which predisposes them to NASH development.[40] This allows for robust induction of a fibrotic phenotype but does not reflect the general human population.

Drugs and pathways targeting LSECs are promising and unexplored methods for treating and preventing NAFLD. Activated LSECs have been shown to be of importance for fibrosis development in animal models.[41] The integration of LSECs into this more complex human spheroid NASH model sheds light on the important regulatory effect of TIMP1 on the formation and degradation of liver fibrosis. This implies that a more complete understanding of the development and degradation of liver fibrosis, including identification of novel drug targets and mediators, will benefit from the use of more complex human liver models, such as the one presented here. In addition, screening for mechanisms of action and efficacy of novel anti-NASH drug candidates would be more complete in models encompassing the major types of liver cells, including highly active LSECs.

AUTHOR CONTRIBUTIONS

Magnus Ingelman-Sundberg and Sander van Riet: Conceived and designed the analysis; Sander van Riet: Collected the data; Sander van Riet, Anais Julien, Andrea Atanasov, and Åsa Nordling: Contributed data or analysis tools; Sander van Riet and Anais Julien: Performed the analysis; Sander van Riet and Magnus Ingelman-Sundberg: Wrote the paper.

ACKNOWLEDGMENTS

The authors thank the Biomedicum Imaging Core Facility for their support with microscopy.

FUNDING INFORMATION

This study was supported by grants from the European Research Council (ERC)–Advanced Grant (AdG) project HEPASPHER (grant agreement 742020), Swedish Research Council (grants 2021–02732 and 2018–05766), and European Research Council (ERC-POC)–grant agreement Project SPHERO-NASH—101123215.

CONFLICTS OF INTEREST

Magnus Ingelman-Sundberg is the cofounder and co-owner of HepaPredict AB. The remaining authors have no conflicts to report.

ORCID

Sander van Riet https://orcid.org/0000–0001–8233–1900
Anais Julien https://orcid.org/0000–0003–0295–605X
Andrea Atanasov https://orcid.org/0009–0008–0660–7192
Magnus Ingelman-Sundberg https://orcid.org/0000–0002–7255–9079

REFERENCES

1. Younossi Z, Stepanova M, Ong JP, Jacobson IM, Bugianesi E, Duseja A, et al. Nonalcoholic steatohepatitis is the fastest growing cause of hepatocellular carcinoma in liver transplant candidates. Clin Gastroenterol Hepatol. 2019;17:748–755.e3.
2. Reimer KC, Wree A, Roderburg C, Tacke F. New drugs for NAFLD: Lessons from basic models to the clinic. Hepatol Int. 2020;14:8–23.
3. Zhang CY, Yuan WG, He P, Lei JH, Wang CX. Liver fibrosis and hepatic stellate cells: Etiology, pathological hallmarks and therapeutic targets. World J Gastroenterol. 2016;22:10512–22.
4. Burra P, Becchetti C, Germani G. NAFLD and liver transplantation: Disease burden, current management and future challenges. JHEP Rep. 2020;2:100192.
5. Wong VWS, Adams LA, de Lédinghen V, Wong GLH, Sookoian S. Noninvasive biomarkers in NAFLD and NASH - Current progress and future promise. Nat Rev Gastroenterol Hepatol. 2018;15:461–78.
6. Iwakiri Y. Endothelial dysfunction in the regulation of cirrhosis and portal hypertension. Liver Int. 2012;32:199–213.
7. Shetty S, Lalor PF, Adams DH. Liver sinusoidal endothelial cells - Gatekeepers of hepatic immunity. Nat Rev Gastroenterol Hepatol. 2018;15:555–67.
8. Deleve LD, Wang X, Guo Y. Sinusoidal endothelial cells prevent rat stellate cell activation and promote reversion to quiescence. Hepatology. 2008;48:920–30.
9. Murphy FR, Issa R, Zhou X, Ratnarajah S, Nagase H, Arthur MJP, et al. Inhibition of apoptosis of activated hepatic stellate cells by tissue inhibitor of metalloproteinase-1 is mediated via effects on matrix metalloproteinase inhibition: Implications for reversibility of liver fibrosis. J Biol Chem. 2002;277:11069–76.
10. Grünwald B, Schoeps B, Krüger A. Recognizing the molecular multifunctionality and interactome of TIMP-1. Trends Cell Biol. 2019;29:6–19.
11. Justo BL, Jasiulionis MG. Characteristics of TIMP1, CD63, and β1-integrin and the functional impact of their interaction in cancer. Int J Mol Sci. 2021;22:9319.
12. Ströbel S, Kostadinova R, Fiaschetti-Egli K, Rupp J, Bieri M, Pawlowska A, et al. A 3D primary human cell-based in vitro model of non-alcoholic steatohepatitis for efficacy testing of clinical drug candidates. Sci Rep. 2021;11:22765.
13. Kozyra M, Johansson I, Nordling Å, Ullah S, Lauschke VM, Ingelman-Sundberg M. Human hepatic 3D spheroids as a model for steatosis and insulin resistance. Sci Rep. 2018;8:14297.
14. Bell CC, Hendriks DFG, Moro SML, Ellis E, Walsh J, Renblom A, et al. Characterization of primary human hepatocyte spheroids as a model system for drug-induced liver injury, liver function and disease. Sci Rep. 2016;6:25187.
15. Hurrell T, Kastrinou-Lampou V, Fardellas A, Hendriks DFG, Nordling Å, Johansson I, et al. Human liver spheroids as a model to study aetiology and treatment of hepatic fibrosis. Cells. 2020;9:964.
16. Trampuž SR, van Riet S, Nordling Å, Ingelman-Sundberg M. The role of CTGF in liver fibrosis induced in 3D human liver spheroids. Cells. 2023;12:302.
17. Stuart T, Butler A, Hoffman P, Hafemeister C, Papalexi E, Mauck WM, et al. Comprehensive integration of single-cell data. Cell. 2019;177:1888–1902.e21.
18. Butler A, Hoffman P, Smibert P, Papalexi E, Satija R. Integrating single-cell transcriptomic data across different conditions, technologies, and species. Nat Biotechnol. 2018;36:411–20.
19. Korsunsky I, Millard N, Fan J, Slowikowski K, Zhang F, Wei K, et al. Fast, sensitive and accurate integration of single-cell data with Harmony. Nat Methods. 2019;16:1289–96.
20. Julien A, Kanagalingam A, Martínez-Sarrà E, Megret J, Luka M, Ménager M, et al. Direct contribution of skeletal muscle mesenchymal progenitors to bone repair. Nat Commun. 2021;12:2860.
21. Gramignoli R, Tahan V, Dorko K, Venkataramanan R, Fox IJ, Ellis ECS, et al. Rapid and sensitive assessment of human hepatocyte functions. Cell Transplant. 2014;23:1545–56.
22. Klöditz K, Tewolde E, Nordling Å, Ingelman-Sundberg M. Mechanistic, functional, and clinical aspects of pro-inflammatory cytokine mediated regulation of ADME gene expression in 3D human liver spheroids. Clin Pharmacol Ther. 2023;114:673–85.
23. Gracia-Sancho J, Caparrós E, Fernández-Iglesias A, Francés R. Role of liver sinusoidal endothelial cells in liver diseases. Nat Rev Gastroenterol Hepatol. 2021;18:411–31.
24. Guilliams M, Bonnardel J, Haest B, Vanderborght B, Wagner C, Remmerie A, et al. Spatial proteogenomics reveals distinct and evolutionarily conserved hepatic macrophage niches. Cell. 2022;185:379–396.e38.
25. Bigg HF, Rowan AD, Barker MD, Cawston TE. Activity of matrix metalloproteinase-9 against native collagen types I and III. FEBS J. 2007;274:1246–55.
26. Guo Q, Furuta K, Islam S, Caporarello N, Kostallari E, Dielis K, et al. Liver sinusoidal endothelial cell expressed vascular cell adhesion molecule 1 promotes liver fibrosis. Front Immunol. 2022;13:983255.
27. Chung KJ, Legaki AI, Papadopoulos G, Gercken B, Gebler J, Schwabe RF, et al. Analysis of the role of stellate cell VCAM-1 in NASH models in mice. Int J Mol Sci. 2023;24:4813.
28. DeLeve LD. Liver sinusoidal endothelial cells in hepatic fibrosis. Hepatology. 2015;61:1740–6.
29. Charles KA, Rivory LP, Brown SL, Liddle C, Clarke SJ, Robertson GR. Transcriptional repression of hepatic cytochrome P450 3A4 gene in the presence of cancer. Clin Cancer Res. 2006;12:7492–7.
30. Siewert E, Bort R, Kluge R, Heinrich PC, Castell J, Jover R. Hepatic cytochrome P450 down-regulation during aseptic inflammation in the mouse is interleukin 6 dependent. Hepatology. 2000;32:49–55.
31. Connolly MK, Bedrosian AS, Malhotra A, Henning JR, Ibrahim J, Vera V, et al. In hepatic fibrosis, liver sinusoidal endothelial cells acquire enhanced immunogenicity. J Immunol. 2010;185:2200–8.
32. Song G, Xu S, Zhang H, Wang Y, Xiao C, Jiang T, et al. TIMP1 is a prognostic marker for the progression and metastasis of colon cancer through FAK-PI3K/AKT and MAPK pathway. J Exp Clin Cancer Res. 2016;35:148.
33. Lachowski D, Cortes E, Rice A, Pinato D, Rombouts K, Del Rio Hernandez A. Matrix stiffness modulates the activity of MMP-9 and TIMP-1 in hepatic stellate cells to perpetuate fibrosis. Sci Rep. 2019;9:7299.
34. Hemmann S, Graf J, Roderfeld M, Roeb E. Expression of MMPs and TIMPs in liver fibrosis - A systematic review with

special emphasis on anti-fibrotic strategies. J Hepatol. 2007; 46:955–75.
35. Fjære E, Andersen C, Myrmel LS, Petersen RK, Hansen JB, Tastesen HS, et al. Tissue inhibitor of matrix metalloproteinase-1 is required for high-fat diet-induced glucose intolerance and hepatic steatosis in mice. PLoS One. 2015;10: e0132910.
36. Yilmaz Y, Eren F. Serum biomarkers of fibrosis and extracellular matrix remodeling in patients with nonalcoholic fatty liver disease: Association with liver histology. Eur J Gastroenterol Hepatol. 2019;31:43–6.
37. Abdelaziz R, Elbasel M, Esmat S, Essam K, Abdelaaty S. Tissue inhibitors of metalloproteinase-1 and 2 and obesity related non-alcoholic fatty liver disease: Is there a relationship. Digestion. 2015;92:130–7.
38. Steinman JB, Salomao MA, Pajvani UB. Zonation in NASH - A key paradigm for understanding pathophysiology and clinical outcomes. Liver Int. 2021;41:2534–46.
39. Kunsch C, Luchoomun J, Grey JY, Olliff LK, Saint LB, Arrendale RF, et al. Selective inhibition of endothelial and monocyte redox-sensitive genes by AGI-1067: A novel antioxidant and anti-inflammatory agent. J Pharmacol Exp Ther. 2004;308:820–9.
40. Luukkonen PK, Nick A, Hölttä-Vuori M, Thiele C, Isokuortti E, Lallukka-Brück S, et al. Human PNPLA3-I148M variant increases hepatic retention of polyunsaturated fatty acids. JCI Insight. 2019;4:e127902.
41. McConnell MJ, Kostallari E, Ibrahim SH, Iwakiri Y. The evolving role of liver sinusoidal endothelial cells in liver health and disease. Hepatology. 2023;78:649–69.

How to cite this article: van Riet S, Julien A, Atanasov A, Nordling Å, Ingelman-Sundberg M. The role of sinusoidal endothelial cells and TIMP1 in the regulation of fibrosis in a novel human liver 3D NASH model. Hepatol Commun. 2024;8: e0374. https://doi.org/10.1097/HC9.0000000000000374